Learning-Based Coordinated Operation of Multiple Microgrids With Hydrogen Systems

A NOVEL BILEVEL FRAMEWORK

xxxxx

By Mohammad H. Shams, Mohammad MansourLakouraj, J. Jay Liu, Mohammad S. Javadi and João P.S. Catalão

Digital Object Identifier 10.1109/MIAS.2022.3214010
Date of current version: 8 December 2022

THIS ARTICLE PROVIDES A FRAMEWORK FOR COORDINATing the operation of multiple microgrids with hydrogen systems in a distribution network considering the uncertainties of wind and solar power generation as well as load demands. The model is based upon a bilevel stochastic programming problem. On the upper level, the distribution system is the leader with a profit-maximization goal, and the microgrids are followers with cost-minimization goals on the lower level. The problem is solved by transforming the model to a single-level model using Karush–Kuhn–Tucker (KKT) conditions and linearized using McCormick's relaxation and Fortuny–Amat techniques. Unlike previous studies, both levels are modeled as scenario-based

1077-2618/22©2022IEEE

stochastic problems. Moreover, the scenarios associated with uncertain variables are obtained from a real data set. After preparing the data set, scenarios are reduced using a machine learning-based clustering approach. An application of the coordinated operation model is developed for a distribution network containing several microgrids. By solving the problem, the optimal amount of power exchange and the clearing price between microgrids and distribution systems are determined. Moreover, the proposed bilevel model made 13% more profit for the distribution system than the centralized model. Also, the effects of integrating hydrogen systems with microgrids on increasing the flexibility of operators are investigated.

Introduction

Background and Aim

Microgrids are defined as *a set of dispersed energy sources within a distribution network to meet the load demand*. From the perspective of the distribution system operator (DSO), a microgrid can perform as a consumer or producer (i.e., a prosumer) that operates in grid-connected and islanding modes [1] (see "Nomenclature").

The usual sources of microgrids are renewable energy sources (RES), storages, microturbines, and diesel generators. In microgrids, energy demands are met with fossil-based electricity unless there is a sustainable source available. Due to this, the energy demand is primarily met by nonrenewable resources, resulting in significant carbon emissions. In the past few years, environmental concerns have arisen due to increased electricity generation by fossil-fueled power plants rather than RES utilization [2].

However, RESs also contribute to microgrids, but they do not compete well enough with fossil fuels because of their high capital costs and volatile nature. Hydrogen, because of its high gravimetric energy density, is becoming increasingly important as a prospective alternative for power generation, gaining vital importance as a potential candidate for energy and power production [3], [4].

Recently, one of the best ways to improve the environment has been the use of hydrogen-based green microgrids. To phase out fossil fuels and limit global warming, hydrogen-based microgrids are expected to be the future, utilizing hydrogen to power components (H2P), power to hydrogen components (P2H), hydrogen-based electric vehicles, and hydrogen storage [5]. On the

Nomenclature

Indices and acronyms:

i	microgrids, $i = 1, 2, \ldots, I$
s	scenarios, $s = 1, 2, \ldots, S$
t	time periods, $t = 1, 2, \ldots, T$
DG	distributed generation
DISCO	distribution system company
DSO	distribution system operator
H2P	hydrogen to power
HS	hydrogen storage
LC	load Curtailment
max/min	upper/lower limits
MG	microgrid
MGO	microgrid operator
PV	photovoltaic units
P2H	power to hydrogen
WT	wind turbine
Δt	time interval

Variables and parameters:

$P_{MG_i}^{t,s}$	purchased power of microgrid i from distribution system at time t and scenario s (MW)
$P_{DA}^{t,s}$	purchased power by DSO from wholesale market at time t and scenario s (MW)
$P_{LC_i}^{t,s}$	load curtailment of microgrid i at time t and scenario s (MW)
$P_{DG_i}^{t,s}$	power generation of DG in microgrid i at time t and scenario s (MW)
$P_{P2H_i}^{t,s}$	consumed power of electrolyzers in microgrid i at time t and scenario s (MW)
$P_{H2P_i}^{t,s}$	generated power of fuel cells in microgrid i at time t and scenario s (MW)
$\pi_{MG_i}^{t,s}$	cleared power price between microgrid i and DSO at time t and scenario s (US$/MWh)
$SOH_i^{t,s}$	state of hydrogen in storage tanks of microgrid i at time t and scenario s (kg)
u	axillary binary variables for the Karush–Kuhn–Tucker approach
μ, λ	Lagrange multipliers
η_i^{P2H}	conversion coefficient of P2H in electrolyzer of microgrid i
η_i^{ELE}	efficiency of electrolyzer of microgrid i
η_i^{FC}	efficiency of fuel cell of microgrid i
LHV	lower heating value of hydrogen (MWh/kg)
$L_i^{t,s}$	electrical demand of microgrid i at time t and scenario s (MW)
M	A large positive constant
$P_{WT_i}^{t,s}$	wind turbines' output power in microgrid i at time t and scenario s (MW)
$P_{PV_i}^{t,s}$	photovoltaic systems' output power in microgrid i at time t and scenario s (MW)
π_{DA}^{t}	purchased power price at time t (US$/MWh)
π_{DG_i}	marginal power price of DG in microgrid i (US$/MWh)
ρ_s	probability of scenario s
$VoLL_i$	value of loss of load of microgrid i (US$/MWh)

other hand, operation planning of power grids is complicated when it comes to uncertainties related to the volatility and limited predictability of solar radiation and wind speed as well as load demands.

Moreover, the decision making between the active distribution system and hydrogen-based microgrids are hierarchical. In contrast to passive distribution systems, the operation problems in this active distribution system are more complex. In this regard, the DSO and microgrid operators (MGOs) need to work together to optimize their respective objectives independently and simultaneously. Therefore, the operation model of microgrids within a distribution system is a collaborative optimization problem.

To deal with the aforementioned complexity, the main goal of this study is to develop a framework for coordinated operation scheduling of multiple microgrids within a distribution system considering system uncertainties. Hence, a bilevel problem formulation is required to define the hierarchical model of the distribution system and microgrids.

Literature Review

Recent studies have suggested that green hydrogen-based networks are among the most effective methods to improve the flexibility and reliability of power systems [6] as dependence on fossil fuels can be eliminated and global warming can be limited through the use of renewable-powered hydrogen systems [5].

A water electrolysis process in electrolyzers can produce green hydrogen from RESs. By using this energy-conversion path, RESs can more likely be integrated into energy systems. Also, this technique can be used as a long-term storage solution to manage demand variability from intermittent energy sources and RESs [7].

In [8], the effects of flexible storage, ramping capability of thermal generators, operating reserve, time indices, and capacity of transmission lines were evaluated based on the frequency of solar curtailments without considering hydrogen systems. The authors of [9] assessed the effects of data centers on mitigating RES curtailments and greenhouse emissions. The practicability of implementing hydrogen-based energy storage and battery technologies was examined using commercial Hybrid Optimization of Multiple Energy Resources (HOMER) software in [10].

Also, an optimal supply-chain planning of an off-grid hydrogen network, including a wind-battery coupling system, was presented in [11]. It considered the uncertainties of hydrogen demand and wind speed. The aforementioned studies did not consider the cooperative operation between the entities and developed a centralized optimization approach.

Some studies have ignored the hierarchical and collaborative nature of decision making when planning the operation of microgrids [12] and multiple-carrier energy systems [13], [14]. In contrast, several studies have focused on bilevel operation modeling of energy systems [15], virtual power plants [16], and microgrids [17], [18]. However, only a few studies have investigated hydrogen-based microgrids in distribution grids. In bilevel problems, capturing the uncertainty is a challenge. The authors of [19] propose a bilevel scenario-based operation planning problem considering the uncertainties of demand, pool prices, and rival retail prices.

According to [20], networked microgrids can be scheduled on a bilevel basis by implementing a two-stage stochastic model. In the first stage, the output power of nondispatchable units is determined, whereas the outputs of units are set in the second stage based on the realized scenarios. Using conditional value at risk, the authors of [21] addressed the decision maker's risk-aversion level and created a data-driven bilevel programming problem. However, generating and reducing scenarios in stochastic modeling is a significant problem.

Most of the power system optimization problems contain a large number of scenarios representing the uncertainties of stochastic variables. These problems are approximated with a selected number of reduced scenarios because of time limitations and computational intensity. In this regard, [22] implements a backward method to reduce the dimension of scenarios set in a stochastic microgrid operation problem. The authors of [23] propose risk-based stochastic scheduling of reserve and energy considering the scenario tree construction and reduction discussed in [24].

Recently, clustering-based machine learning algorithms have been used in studies. In [25], *k*-means clustering is implemented in multimicrogrids planning with renewables' uncertainty. Moreover, [26] presents an unsupervised clustering method for scenario reduction in stochastic optimization of renewable energy plants. Finally, Table 1 summarizes the differences between the current work and previous studies.

Contributions and Article Organization

To overcome the research gap, this study uses a bilevel stochastic model to evaluate the operation scheduling of microgrids based on hydrogen energy while taking the uncertainties of demand, solar, and wind power into consideration. The innovative contributions of this article are as follows:

- This article proposes a novel mathematical model for bilevel stochastic short-term planning of microgrids within distribution systems. In contrast to the earlier studies such as [19] and [20], both upper- and lower-level problems are formulated as a scenario-based stochastic model.
- A set of realistic scenarios for load demand, wind, and solar power has been incorporated for stochastic problem modeling. Then, a data-driven approach is carried out to reduce the number of initial scenarios to the most accurate and probable scenarios using the *k*-means clustering method.

Table 1. Comparison of relevant studies and this article

Reference	Power Market	Multiple Microgrid	Hydrogen System	Linearized Model	Scenario-Reduction Technique	Problem Type
[12]	✗	✓	✗	✓	N/A	Deterministic MILP
[13]	✗	✗	✗	✓	N/A	Robust optimization
[14]	✗	✗	✗	✓	Backward	Risk averse
[16]	✓	✓	✗	✓	N/A	Chance bilevel
[22]	✗	✗	✗	✓	Backward	Risk averse
[27]	✓	✓	✗	✓	Forward	Risk-based bilevel
[28]	✓	✓	✓	✓	Forward	Stochastic bilevel
[29]	✗	✗	✓	✗	N/A	Deterministic MILP
This article	✓	✓	✓	✓	Machine learning	Stochastic bilevel

N/A: not applicable.

- In comparison to other previous studies such as [27] and [30], microgrids use more resources, like hydrogen systems with electrolyzers, fuel cells, and hydrogen storage systems, as during the DSO operation, the MGO should be able to participate with greater flexibility.

A preliminary study was presented in [28], which significantly differs from this one in terms of machine learning-based scenario preparation and reduction. Also, the uncertainty modeling in the bilevel problem modeling was changed, several new case studies have been defined, and new observations have been obtained. The other sections of this article are listed here. The "Proposed Bilevel Problem And formulation" section describes the bilevel problem formulation. Uncertainty modeling is determined in the "Uncertainty Modeling" section. The "Solution Methodology" section investigates the solution methodology. The "Case Study and Description of Test System" section provides the case study and the description of the test system. Results and sensitivity analysis are provided in the "Results and Discussion" section. Finally, the "Conclusion" section concludes the article.

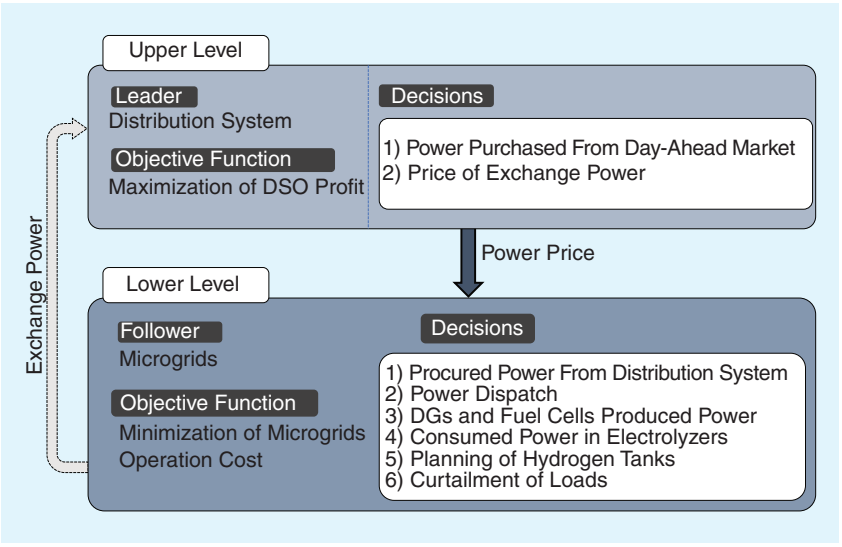

FIGURE 1. A framework of the proposed bilevel stochastic problem.

Proposed Bilevel Problem and Formulation

In this study, it is assumed that the microgrids and the distribution systems have different owners. So, the goal of this model is to maximize the DSO's profit through bilevel programming, whereas microgrids minimize the operating costs to serve their loads. This model is presented in Figure 1.

Microgrid power prices and power purchased from the day-ahead market are decision variables at the upper level that determine the distribution system's profit. In the wholesale electricity market, the distribution system is assumed to be a price taker that cannot affect the day-ahead prices. The lower levels are assigned to MGOs and represent the amounts of power exchanged with the distribution system, the produced power from distributed generation, and the load curtailments. Hydrogen systems, including electrolyzers, fuel cells, and hydrogen tanks, are also scheduled. The framework involves coordination of the operation of multiple microgrids within a distribution network to satisfy the goals of both entities. In this regard, microgrids and distribution systems will exchange power at a cleared price and amount. The objectives of both levels are determined in the following.

Upper Level: Operation Model of the DSO

The stochastic operation model of the DSO within the upper level is determined in this section. The objective function in (1) defines the upper-level problem with the constraints in (2)–(4). The first term in (1) is the revenue from the microgrids' sale of power, and the second term is the cost of purchasing power from the wholesale power market for each scenario. The microgrid's power prices are kept within a reasonable range by (2). According to (3), the DSO is limited in the amount of power purchased on the day-ahead market. Also, (4) ensures the balance between bought and sold power.

Maximize Profit:

$$\rho_s \sum_{s=1}^{S} \sum_{t=1}^{T} \sum_{i=1}^{I} \{P_{\mathrm{MG}_i}^{t,s} \,.\, \pi_{\mathrm{MG}_i}^{t,s} - P_{DA}^{t,s} \,.\, \pi_{DA}^{t}\} \,\Delta t \tag{1}$$

$$0 \le \pi_{\mathrm{MG}_i}^{t,s} \le \pi_{\mathrm{MG}}^{\max} \tag{2}$$

$$0 \le P_{DA}^{t,s} \le P_{DA}^{\max} \tag{3}$$

$$\sum_{i=1}^{I} P_{\mathrm{MG}_i}^{t,s} \le P_{DA}^{t,s}. \tag{4}$$

Lower Level: Operation Model of the MGO

The operation model of the MGO within the lower level is determined in this section. As shown in (5), the lower-level problem has a cost-minimization objective function.

The expected cost of purchasing power from the DSO is shown in the first term of (5). The expected cost of the obtained power from the distributed generations (DGs) and the loads' curtailments are indicated in the second and third terms, respectively. Constraint (6) describes the allowable power exchange between microgrids and the distribution system.

The generation limits of DGs are guaranteed in (7). Equation (8) ensures the permissible amount of electrical load curtailment. The power balance at each microgrid is defined in (9). The constraints of (10)–(12) define the hydrogen storage tanks' limitations. In (10), the hydrogen balance is described. In (11), the state of hydrogen in storage tanks is limited, and (12) maintains the same level of hydrogen in tanks at the start and the end of the scheduling period. In (10), the conversion coefficients of electrolyzers and fuel cell units are defined as $\eta_i^{P2H} = \eta_i^{\mathrm{ELE/FC}}/\mathrm{LHV}$, where $\eta_i^{\mathrm{ELE/FC}}$ and LHV are the efficiency of electrolyzers or fuel cells, and lower heating value of hydrogen, respectively [29]. In (9) and (10), if the value of $P_{P2H_i}^{t,s}$ is obtained positive, that means the electrolyzers are utilized, and if the value found negative, that implies that fuel cells are used in the operation scheduling. Equation (13) limits the amount of generated power and hydrogen in electrolyzers and fuel cells, respectively. In (6)–(13), μ and λ are Lagrange multipliers that will be used in the following for the problem solution methodology.

Minimize Cost:

$$\rho_s \sum_{s=1}^{S} \sum_{t=1}^{T} \sum_{i=1}^{I} \{P_{\mathrm{MG}_i}^{t,s} \,.\, \pi_{\mathrm{MG}_i}^{t,s} + P_{\mathrm{DG}_i}^{t,s} \,.\, \pi_{\mathrm{DG}_i} + P_{\mathrm{LC}_i}^{t,s} \,.\, VoLL_i\} \,\Delta t \tag{5}$$

$$-P_{\mathrm{MG}}^{\max} \le P_{\mathrm{MG}_i}^{t,s} \le P_{\mathrm{MG}}^{\max} : \mu_{2,i}^{t,s}, \mu_{1,i}^{t,s} \tag{6}$$

$$P_{\mathrm{DG}_i}^{\min} \le P_{\mathrm{DG}_i}^{t,s} \le P_{\mathrm{DG}_i}^{\max} : \mu_{4,i}^{t,s}, \mu_{3,i}^{t,s} \tag{7}$$

$$0 \le P_{\mathrm{LC}_i}^{t,s} \le P_{\mathrm{LC}_i}^{\max} : \ \mu_{6,i}^{t,s}, \mu_{5,i}^{t,s} \tag{8}$$

$$P_{\mathrm{MG}_i}^{t,s} + P_{\mathrm{DG}_i}^{t,s} - P_{P2H_i}^{t,s} + P_{\mathrm{WT}_i}^{t,s} + P_{\mathrm{PV}_i}^{t,s} = L_i^{t,s} - P_{LC_i}^{t,s} \quad : \lambda_{1,i}^{t,s} \text{ unrestricted} \tag{9}$$

$$\mathrm{SOH}_i^{t,s} = \mathrm{SOH}_i^{t-1,s} + \eta_i^{P2H} \cdot P_{P2H_i}^{t,s} : \lambda_{2,i}^{t,s} \text{ unrestricted} \tag{10}$$

$$\mathrm{SOH}_i^{\min} \le \mathrm{SOH}_i^{t,s} \le \mathrm{SOH}_i^{\max} : \mu_{8,i}^{t,s}, \mu_{7,i}^{t,s} \tag{11}$$

$$\mathrm{SOH}_i^{1,s} = \mathrm{SOH}_i^{T,s} : \lambda_{3,i}^{t,s} \text{ unrestricted} \tag{12}$$

$$-P_{P2H_i}^{\max} \le P_{P2H_i}^{t,s} \le P_{P2H_i}^{\max} : \ \mu_{10,i}^{t,s}, \mu_{9,i}^{t,s}. \tag{13}$$

Uncertainty Modeling

MGOs face several uncertainties during the scheduling process. A scenario-based stochastic problem is defined in this study where the power generation from wind and solar energy, as well as loads, are considered uncertain parameters. The following sections provide an overview of scenario preparation and reduction techniques.

Scenario Preparation

To model the uncertainties, the real daily data of wind and solar power generation as well as load demand of California independent system operator (CAISO) in 2019–2020 have been utilized [31]. The data are sorted for 1-h intervals to maintain consistency because they were at different minute intervals.

Scenario Reduction With Machine Learning

A vector of scenarios is obtained for each uncertain variable, such as solar, wind, and load. The vector consists of 730 daily scenarios for all variables that are prepared for the operation analysis. However, the computation time of stochastic problems is highly dependent on the number of scenarios. Therefore, an efficient scenario-reduction algorithm is needed for reducing the size of the data set to make the problem tractable for real-world applications considering the stochasticity of the relevant variables.

In our previous study [28], the scenario generation and reduction tool with the forward method in general algebraic modeling system (GAMS) software [32] was used to shrink the set of initial scenarios. However, in this study, one of the most efficient unsupervised clustering methods is implemented for reducing the scenarios' dimension, known as the k-*means clustering algorithm*.

An unsupervised *k*-means algorithm categorizes a massive number of scenarios into clusters where scenarios are similar in some manner in each group. In fact, the scenarios of each cluster have some similar features. For this

clustering algorithm, the centroid is defined, which is the center of the cluster.

Initially, the number of clusters or centroids is defined in the algorithm. The data set $Z = \{z_1, z_2, z_3, \ldots, z_i, \ldots, z_k\}$ is given to the *k*-means model. $z_i \in R^n$ indicates data with the dimension of n, which is equal to 24. The algorithm classifies k scenarios to m different classes, specified with c_m.

In each class, the cluster center ∂_m is used in squared Euclidean distance as the similarity criteria. This criterion measures the distance between the centroid and the scenario of a cluster [33]. The mathematical representation of the Euclidean distance is given as (14).

$$L(c_m) = \sum_{z_i \in c_m} \| z_i - \partial_m \|^2. \tag{14}$$

The main goal of the clustering is to minimize the distance in whole classes as (15).

$$L(C) = \sum_{m=1}^{M} L(c_m) = \sum_{m=1}^{M} \sum_{i=1}^{k} d_{mi} \| z_i - \partial_m \|^2. \tag{15}$$

where

$$d_{mi} = \begin{cases} 0, & z_i \notin c_m \\ 1, & z_i \in c_m \end{cases}. \tag{16}$$

The clustering *k*-means algorithm contains the following steps:

- defining m as the number of clusters
- locating m centroids randomly
- calculating the distance between centroids and samples
- assigning each sample (point) to the nearest center
- updating the centroid's location to the average value of points related to centroids
- performing sufficient iterations to minimize the Euclidean distance and satisfy the set criteria.

With the aim of the proposed unsupervised learning method, five scenarios are obtained for each uncertain variable. The scenarios are grouped based on their label numbers, and the probability of each vector consisting of three combined variables (such as load, solar, and wind power) is calculated with the average probability.

Solution Methodology

Methods of straightforward optimization will not be able to solve the proposed bilevel problem. So, we should transform the problem into a linear, single-level problem. Step one is to apply KKT-optimal conditions to replace the lower-level MGs' operation problem in (5)–(13). So, as (17)–(31), single-level mathematical programming with equilibrium constraints (MPECs) is attained [34].

In the MPECs, constraints (17)–(21) are stationarity conditions, (6)–(13) are the primal feasibility conditions, and (22)–(31) are the complementary slackness conditions, respectively.

$$\pi^{t,s}_{\mathrm{MG}_i} - \mu^{t,s}_{1,i} + \mu^{t,s}_{2,i} - \lambda^{t,s}_{1,i} = 0 \tag{17}$$

$$\pi_{\mathrm{DG}_i} - \mu^{t,s}_{3,i} + \mu^{t,s}_{4,i} - \lambda^{t,s}_{1,i} = 0 \tag{18}$$

$$VoLL_i - \mu^{t,s}_{5,i} + \mu^{t,s}_{6,i} - \lambda^{t,s}_{1,i} = 0 \tag{19}$$

$$-\mu^{t,s}_{7,i} + \mu^{t,s}_{8,i} + \lambda^{t-1,s}_{2,i} - \lambda^{t,s}_{2,i} + \lambda^{T,s}_{3,i} - \lambda^{1,s}_{3,i} = 0 \tag{20}$$

$$-\mu^{t,s}_{9,i} + \mu^{t,s}_{10,i} + \eta^{P2H}_i \cdot \lambda^{t,s}_{2,i} + \lambda^{t,s}_{1,i} = 0 \tag{21}$$

$$0 \le (P^{t,s}_{\mathrm{MG}_i} + P^{\max}_{\mathrm{MG}}) \perp \mu^{t,s}_{1,i} \ge 0 \tag{22}$$

$$0 \le (P^{\max}_{\mathrm{MG}} - P^{t,s}_{\mathrm{MG}_i}) \perp \mu^{t,s}_{2,i} \ge 0 \tag{23}$$

$$0 \le (P^{t,s}_{\mathrm{DG}_i} - P^{\min}_{\mathrm{DG}_i}) \perp \mu^{t,s}_{3,i} \ge 0 \tag{24}$$

$$0 \le (P^{\max}_{\mathrm{DG}_i} - P^{t,s}_{\mathrm{DG}_i}) \perp \mu^{t,s}_{4,i} \ge 0 \tag{25}$$

$$0 \le P^{t,s}_{\mathrm{LC}_i} \perp \mu^{t,s}_{5,i} \ge 0 \tag{26}$$

$$0 \le (P^{\max}_{\mathrm{LC}_i} - P^{t,s}_{\mathrm{LC}_i}) \perp \mu^{t,s}_{6,i} \ge 0 \tag{27}$$

$$0 \le (\mathrm{SOH}^{t,s}_i - \mathrm{SOH}^{\min}_i) \perp \mu^{t,s}_{7,i} \ge 0 \tag{28}$$

$$0 \le (\mathrm{SOH}^{\max}_i - \mathrm{SOH}^{t,s}_i) \perp \mu^{t,s}_{8,i} \ge 0 \tag{29}$$

$$0 \le (P^{t,s}_{P2H_i} + P^{\max}_{P2H_i}) \perp \mu^{t,s}_{9,i} \ge 0 \tag{30}$$

$$0 \le (P^{\max}_{P2H_i} - P^{t,s}_{P2H_i}) \perp \mu^{t,s}_{10,i} \ge 0. \tag{31}$$

Afterward, it is necessary to linearize both the objective function and constraints. The term $P^{t,s}_{\mathrm{MG}_i} \cdot \pi^{t,s}_{\mathrm{MG}_i}$ in the objective function (1) is a nonlinear expression, which is linearized by defining an auxiliary variable $q^{t,s}_i = P^{t,s}_{\mathrm{MG}_i} \cdot \pi^{t,s}_{\mathrm{MG}_i}$ and satisfying constraints (33)–(37) using McCormick's relaxation approach [35].

Moreover, constraints (22)–(31) are nonlinear because of the form of $a \perp b$, which defines that the product of a and b must be zero. So, we have $a \ge 0$, $b \ge 0$, and $a.b = 0$. The Fortuny–Amat method can be used to linearize these equations as (43)–(53) [36]. Finally, (32)–(53) demonstrate the linear single-level objective function and constraints of the proposed stochastic bilevel model.

$$\rho_s \sum_{s=1}^{S} \sum_{t=1}^{T} \sum_{i=1}^{I} \{q^{t,s}_i - P^{t,s}_{DA} \cdot \pi^{t}_{DA}\} \tag{32}$$

subject to

$$q^{t,s}_i \ge P^{t,s}_{\mathrm{MG}_i} \cdot \pi^{\max}_{\mathrm{MG}} + P^{\max}_{\mathrm{MG}} \cdot \pi^{t,s}_{\mathrm{MG}_i} - P^{\max}_{\mathrm{MG}} \cdot \pi^{\max}_{\mathrm{MG}} \tag{33}$$

$$q^{t,s}_i \le P^{t,s}_{\mathrm{MG}_i} \cdot \pi^{\max}_{\mathrm{MG}} \tag{34}$$

$$q^{t,s}_i \le P^{\max}_{\mathrm{MG}} \cdot \pi^{t,s}_{\mathrm{MG}_i} \tag{35}$$

$$0 \le P^{t,s}_{\mathrm{MG}_i} \le P^{\max}_{\mathrm{MG}} \tag{36}$$

$$0 \le \pi^{t,s}_{\mathrm{MG}_i} \le \pi^{\max}_{\mathrm{MG}} \tag{37}$$

(2)–(4), (6)–(13)

$$\pi^{t,s}_{\mathrm{MG}_i} - \mu^{t,s}_{1,i} + \mu^{t,s}_{2,i} - \lambda^{t,s}_{1,i} = 0 \tag{38}$$

$$\pi_{\mathrm{DG}_i} - \mu^{t,s}_{3,i} + \mu^{t,s}_{4,i} - \lambda^{t,s}_{1,i} = 0 \tag{39}$$

$$VoLL_i - \mu^{t,s}_{5,i} + \mu^{t,s}_{6,i} - \lambda^{t,s}_{1,i} = 0 \tag{40}$$

$$-\mu^{t,s}_{7,i} + \mu^{t,s}_{8,i} + \lambda^{t-1,s}_{2,i} - \lambda^{t,s}_{2,i} = 0 \tag{41}$$

$$-\mu^{t,s}_{9,i} + \mu^{t,s}_{10,i} + \eta^{P2H}_i \cdot \lambda^{t,s}_{2,i} + \lambda^{t,s}_{1,i} = 0 \tag{42}$$

$$\mu^{t,s}_{x,i} \le M \cdot (1 - u^{t,s}_{x,i}) \ \forall x = 1, 2, \ldots, 10 \tag{43}$$

$$P^{t,s}_{\mathrm{MG}_i} + P^{\max}_{\mathrm{MG}} \le M \cdot u^{t,s}_{1,i} \quad (44)$$

$$-P^{t,s}_{\mathrm{MG}_i} + P^{\max}_{\mathrm{MG}} \le M \cdot u^{t,s}_{2,i} \quad (45)$$

$$P^{t,s}_{\mathrm{DG}_i} - P^{\min}_{\mathrm{DG}_i} \le M \cdot u^{t,s}_{3,i} \quad (46)$$

$$-P^{t,s}_{\mathrm{DG}_i} + P^{\max}_{\mathrm{DG}_i} \le M \cdot u^{t,s}_{4,i} \quad (47)$$

$$P^{t,s}_{\mathrm{LC}_i} \le M \cdot u^{t,s}_{5,i} \quad (48)$$

$$-P^{t,s}_{\mathrm{LC}_i} + P^{\max}_{\mathrm{LC}_i} \le M \cdot u^{t,s}_{6,i} \quad (49)$$

$$SOH^{t,s}_i - SOH^{\min}_i \le M \cdot u^{t,s}_{7,i} \quad (50)$$

$$-SOH^{t,s}_i + SOH^{\max}_i \le M \cdot u^{t,s}_{8,i} \quad (51)$$

$$P^{t,s}_{P2H_i} + P^{\max}_{P2H_i} \le M \cdot u^{t,s}_{9,i} \quad (52)$$

$$-P^{t,s}_{P2H_i} + P^{\max}_{P2H_i} \le M \cdot u^{t,s}_{10,i}. \quad (53)$$

Case Study and Description of Test System

Four microgrids within a distribution system are used as a case study for evaluating the proposed day-ahead operation scheduling model using a bilevel problem, as shown in Figure 2. The components of the microgrids are DGs, solar photovoltaic systems, and wind turbines.

Moreover, Figure 3 shows how all microgrids are connected to the hydrogen systems. Hydrogen systems include water electrolyzer units (i.e., P2H units), fuel cell units (i.e., H2P units), and hydrogen storage tanks. So, the surplus power can be converted to hydrogen using electrolyzers and stored in hydrogen tanks. Consequently, the stored hydrogen can be converted to power using fuel cells when needed.

The MGO becomes more flexible with this model because electricity can be converted to hydrogen by electrolyzers in lower-price or lower-demand hours and kept in hydrogen tanks. Then, hydrogen can be converted back into power using fuel cells during hours of high demand or high price.

The electrical loads in microgrids are served by the power sources, including DGs, solar systems, and wind turbines, while the distribution system can supply the remaining load.

The upper range for the power exchange between distribution systems and microgrids is 10 MW, while the maximum power price from the distribution system to microgrids is constrained to US$60/MWh.

The limitation of the distribution system to purchase power from the wholesale electricity market is set to 40 MW. The value of loss of load is considered US$100/MWh, and the share of each microgrid from the whole system's load is 25%.

Table 2 determines the components of each microgrid and their characteristics, including distributed generations, solar systems, and wind turbines. The specifications of the hydrogen systems are listed in Table 3. It is considered that all the microgrids have a hydrogen system with the same characteristics.

Considering the uncertainties, 730 real scenarios for demands, wind, and solar power in each period are utilized from the CAISO. Using the *k*-means clustering algorithm, the prepared initial scenarios are reduced to five to decrease the

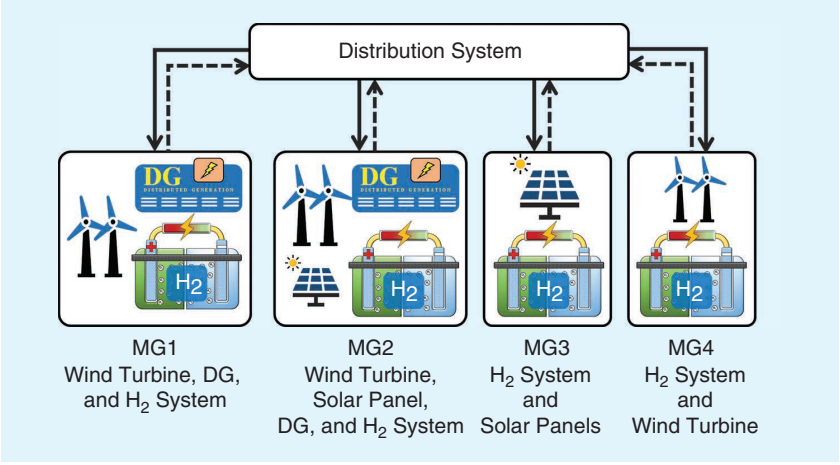

FIGURE 2. A model of the test microgrids and distribution system. MG: microgrid; DG: distributed generation.

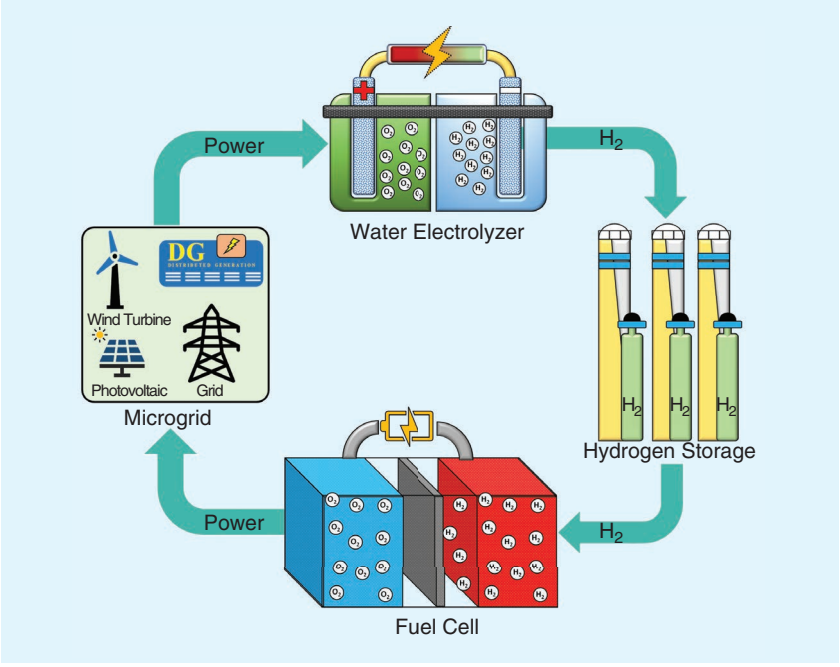

FIGURE 3. The integration of a hydrogen system with the microgrids. DG: distributed generation.

computation time. Figure 4 illustrates the scenarios of electrical demand, wind, and solar power. The dashed line in Figure 4(d) is the day-ahead electricity price from the wholesale electricity market.

Results and Discussion

The coordinated day-ahead operation model of microgrids in the distribution system is formulated as a mixed-integer linear programming (MILP) problem and solved by the CPLEX solver, which runs in the GAMS environment [37]. The results are presented considering the following case studies:

Case 1

Coordinated optimal operation of microgrids and the distribution system using the proposed bilevel approach. In this case, the optimal power exchange and price between the microgrids and distribution system will be cleared. So any change from the optimal points may result in profit reduction or operation cost increase.

Table 2. Characteristics of resources in microgrids

Diesel Generator	π_{DG} (US$/MWh)	P_{DG}^{min} (MW)	P_{DG}^{max} (MW)
MG1	55	0	5
MG2	45	0	5
Wind turbine	$P_{WT,rated}$ (MW)	Solar system	$P_{PV,rated}$ (MW)
MG1	2	MG2	5
MG4	2	MG3	5

MG: microgrid.

Table 3. Characteristics of the hydrogen systems

Hydrogen System	$SOH_i^{min-max}$ (kg)	η_i^{ELE-FC} (%)	$P_{P2H-H2P}^{max}$ (MW)	*LHV* (MWh/kg)
All MGs	0–100	47–68	1–1	0.033

MG: microgrid; LHV: lower heating value.

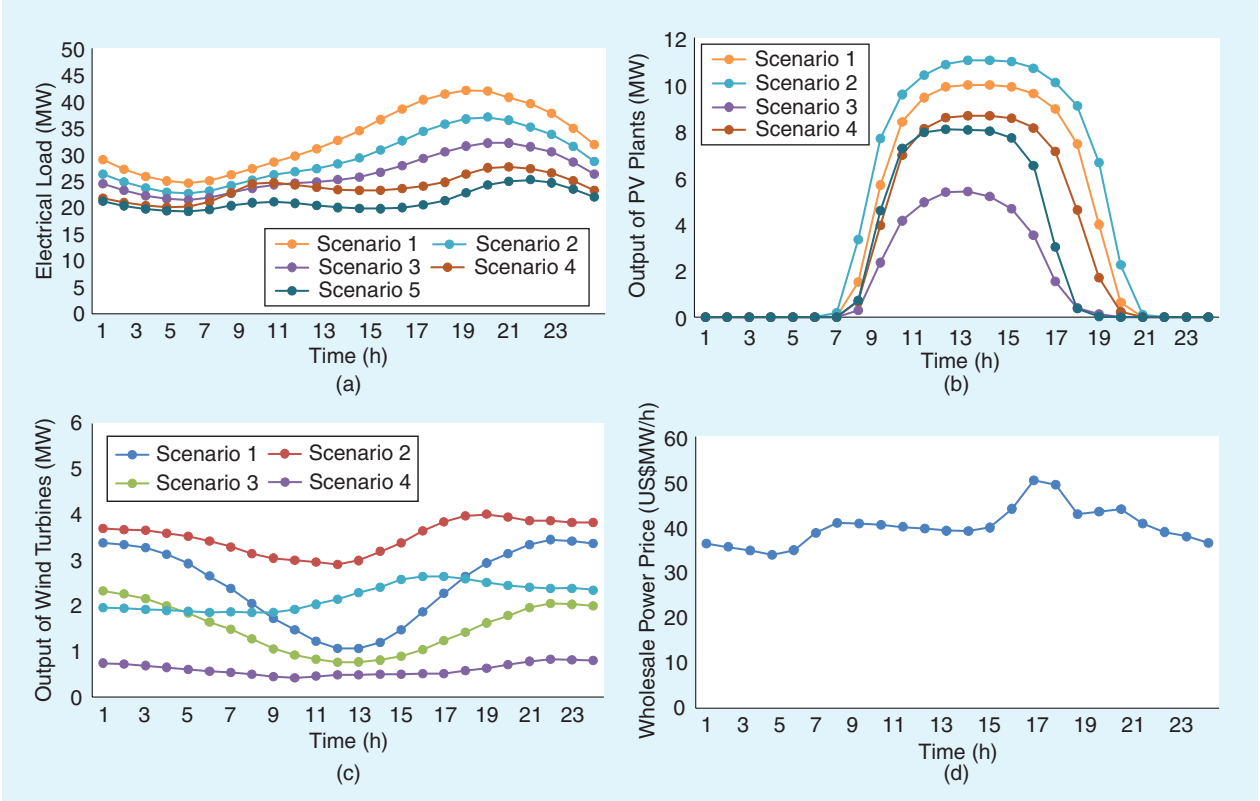

FIGURE 4. The reduced scenarios of (a) electrical demand, (b) wind power, (c) solar power, and (d) wholesale electricity market price. PV: photovoltaic.

Table 4. Distribution system profit analysis

	Case 1 (US$)			Case 2 (US$)		
Scenario Number	Revenue	Cost	Profit	Revenue	Cost	Profit
1	34,502	25,486	9,016	29,624	25,301	4,323
2	23,370	20,120	3,249	23,772	20,121	3,651
3	27,612	22,472	5,139	26,362	22,462	3,900
4	21,220	18,865	2,355	22,400	18,856	3,543
5	18,674	15,569	3,104	18,583	15,561	3,022
Expected	24,112	20,000	4,112	23,596	19,966	3,630

Table 5. Operation costs of the microgrids in the scenarios

Scenario Number	MGO Cost (US$) Case 1	MGO Cost (US$) Case 2	Probability
1	34,711	31,381	0.151
2	23,381	24,786	0.173
3	27,612	27,448	0.164
4	21,220	23,341	0.317
5	18,674	19,299	0.193
Expected	24,145	24,652	—

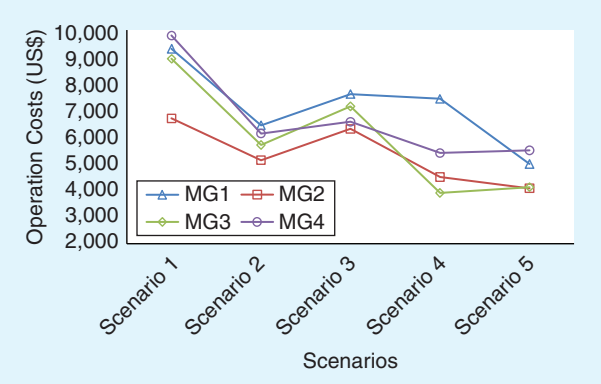

FIGURE 5. Operation cost of the microgrids in the scenarios. MG: microgrid.

Case 2

Centralized optimal operation of microgrids in the distribution system with a given power exchange price. In this case, the objective function is the microgrids' cost minimization, and an average power price of US$50/MWh is considered as a given power exchange price between the microgrids and the distribution system. So, the optimal operation of microgrids and the amount of power exchange between microgrids and the distribution system will be cleared.

The revenue, cost, and profit of the distribution system in five scenarios and two case studies are demonstrated in Table 4. As exposed, in case 1, the coordinated operation provided more revenue and, therefore more profit as compared to case 2. However, the results in case 2 depend on the power exchange price between the microgrids and the distribution system. Furthermore, it is shown that scenario 1 makes the most amount of profit, whereas scenario 4 makes the least. Additionally, as wholesale market prices affect the operating costs of the distribution system, the expected operation costs are almost similar in both cases.

The computation time for both case studies was less than a minute. However, the computation time for the single-level nonlinear model was more than an hour with different results using nonlinear solvers. The bilevel model consists of 19,441 equations, 14,041 single variables, and 4,800 discrete variables.

The operation costs of all microgrids in scenarios and cases are demonstrated in Table 5. As shown, the highest operation cost is observed in scenario 1, and the least occurred in scenario 5. As the expected operation cost of the microgrids in both cases are almost equal, it can be concluded that the proposed coordinated approach in case 1 managed to operate the system as efficiently as in case 2.

Moreover, Figure 5 demonstrates the operation costs of each microgrid in scenarios in case 1. As displayed, the first microgrid (i.e., MG1) has the highest operation cost, while the second microgrid (i.e., MG2) has the lowest operation cost. This is basically because of the type and capacity of resources in microgrids. For example, in the second microgrid, there exists a low-cost distributed generation as well as a high-capacity solar photovoltaic system, which results in the lowest operation cost.

The hourly offered power price to the microgrids by the distribution system is shown in Figure 6. For all hours, the cleared power prices are almost the same and are optimally obtained as 55, 45, 60, and US$60/MWh for MG1, MG2, MG3, and MG4, respectively.

In MG1 and MG2, there are DGs with a marginal price of 45 and US$55/MWh, respectively, which are desired to

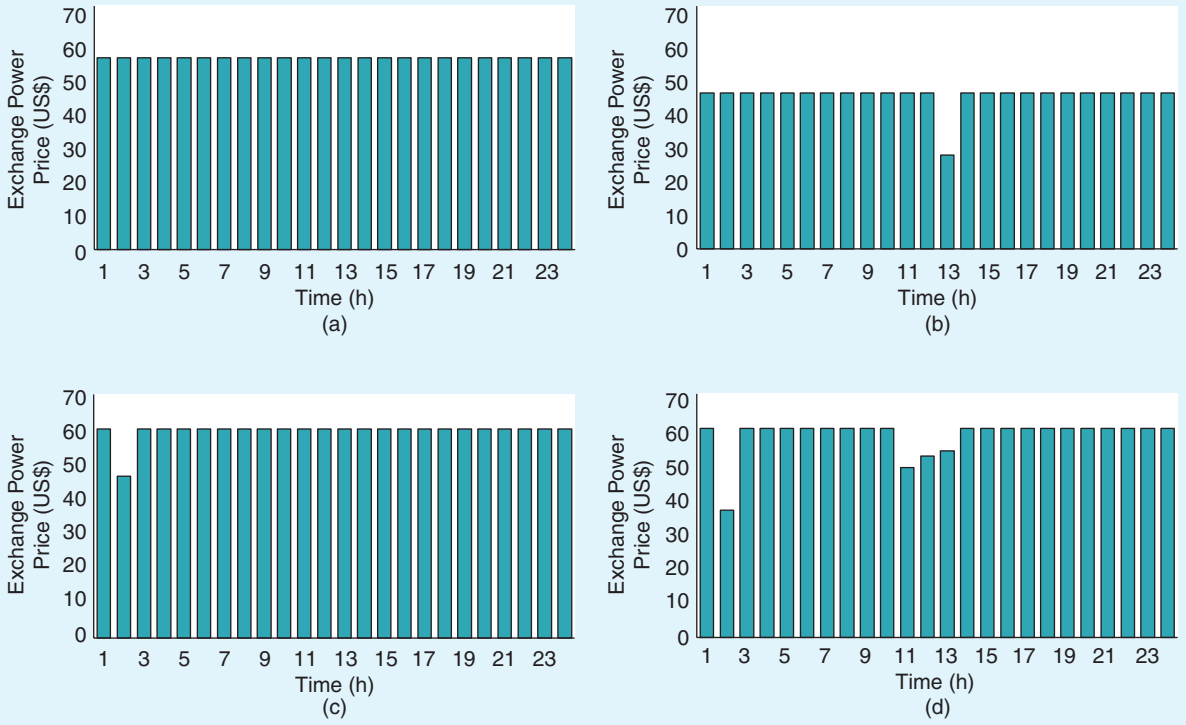

FIGURE 6. Purchased power price from the distribution system by the microgrids. MG: microgrid. (a) MG1, (b) MG2, (c) MG3, and (d) MG4.

be employed rather than buying power from the distribution system when needed. In other words, the clearing power price between these two microgrids and the distribution system cannot be more than the DGs' marginal price.

Contrary to MG1 and MG2, the clearing prices for MG3 and MG4 are higher and set to US$60/MWh, which is the highest power price within the acceptable range between the distribution system and all microgrids. This is because MG3 and MG4 do not have any resources to feed the loads in the high-demand hours, and their MGOs have to procure the energy from the distribution system with the highest possible power exchange price, which is US$60/MWh.

On the other hand, the acquired energy by DSO from the wholesale power market in cases 1 and 2 are represented in Figure 7. As shown, the purchased power in case 2 is less than in case 1. As in case 1, the upper-level objective function is the DSO's profit maximization: the optimization procedure tries to increase the power sold to the microgrids.

However, the second level of the problem is the microgrids' cost minimization, which results in the optimum power exchange for both microgrids and the distribution system, as shown in Figure 7.

Alternatively, in case 2, as the objective is to minimize the operation costs of the microgrids, less power will be procured from the DSO, resulting in less power purchased from the wholesale market.

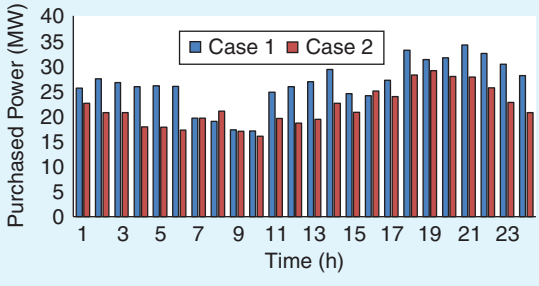

FIGURE 7. Purchased power by the DSO from the wholesale market.

To analyze the performance of the hydrogen systems, Figures 8 and 9 illustrate the weight of hydrogen in the storage tanks and the amount of P2H and H2P, respectively, for the first scenario in all microgrids.

As shown Figure 8, the weight of hydrogen in storage tanks is increasing to store the produced hydrogen in low-demand hours (i.e., hours 1–6 and 11–14) and decreasing to withdraw the hydrogen at hours with high demand in MG1, MG3, and MG4. In these microgrids, at hours 19–24, as the power demand is low, the hydrogen systems are not utilized, and the storage tanks are empty. However, in MG2, the hydrogen system is incorporated by the MGO to add more flexibility at the late hours of the day. In peak hours, fuel cells convert the stored H2P and reduce the state of hydrogen in storage tanks. Then again, in off-

peak hours, electrolyzers convert the P2H and increase the state of hydrogen in storage tanks.

The amount of converted P2H using electrolyzers and H2P using fuel cells in the first scenario is depicted in Figure 9. The positive values imply that power is converted to hydrogen in electrolyzers, and the negative values represent that hydrogen is converted to power in the fuel cells. As shown, for all the microgrids except MG2, in hours 1–6 and 11–14, the electrolyzers are working to produce hydrogen, and in hours 7–10 and 15–20, the fuel cells are working to produce power using hydrogen, and finally, in hours 21–24, neither the electrolyzers nor the fuel cells are working. For MG2, in hours 19–24, fuel cells are working to feed the loads.

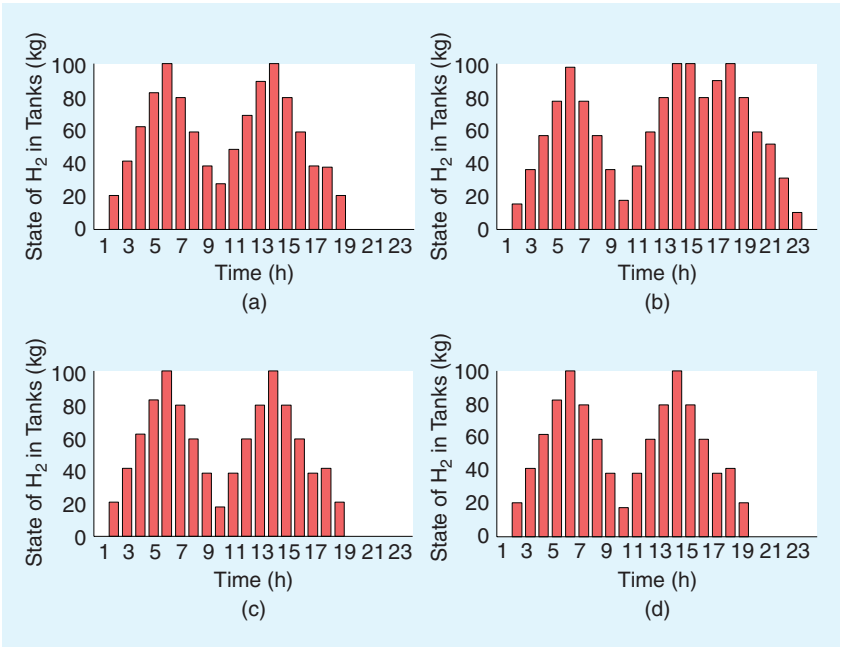

FIGURE 8. The state of hydrogen (H_2) in the H_2 tanks in the microgrids. MG: microgrid. (a) MG1, (b) MG2, (c) MG3, and (d) MG4.

It can be understood that the hydrogen system enhances the flexibility of the system to manage the oversupply of renewable resources. The hydrogen system increases the system's reliability to feed the loads in case of peak hours.

Figure 10 demonstrates the power dispatch of the microgrids in scenario 1. As presented, the purchased power from the DSO in all microgrids has the largest share of power procurement. As the upper-level objective function maximizes

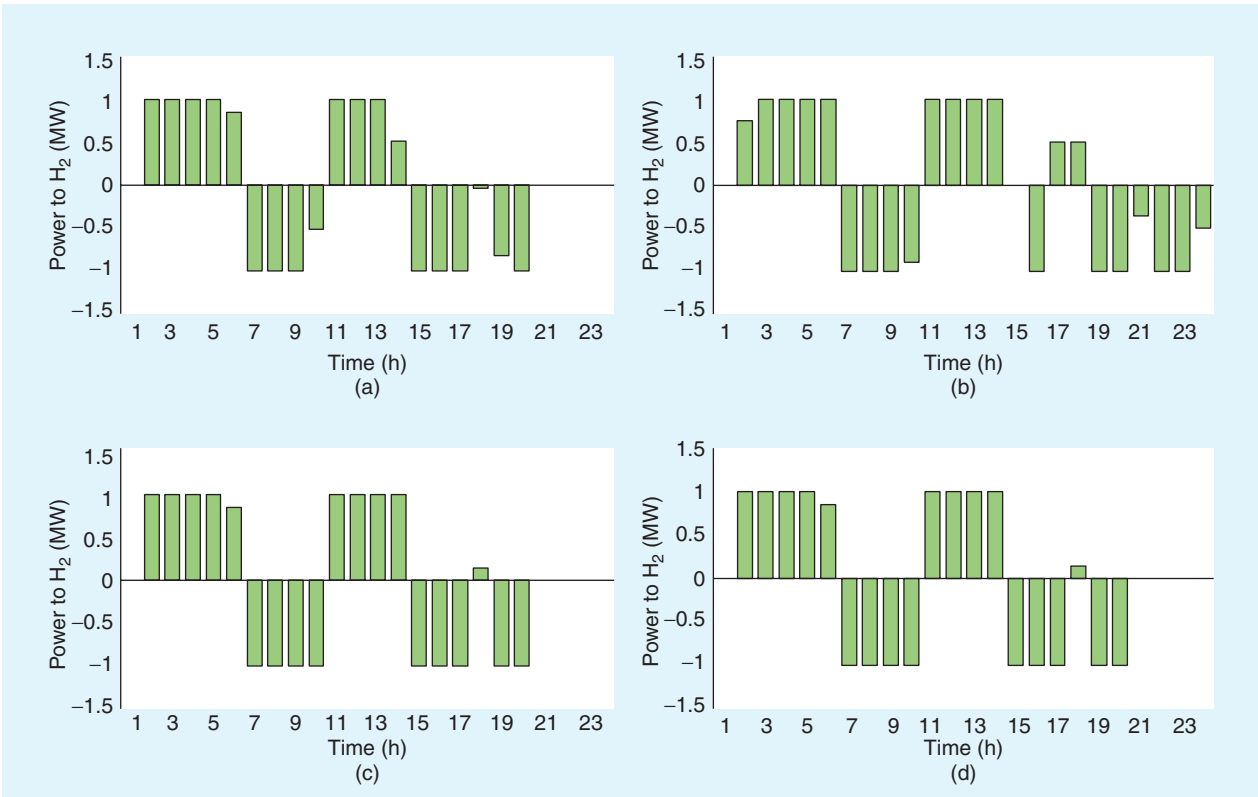

FIGURE 9. The amount of P2H in the electrolyzers and hydrogen (H_2) to power in the fuel cells. MG: microgrid. (a) MG1, (b) MG2, (c) MG3, and (d) MG4.

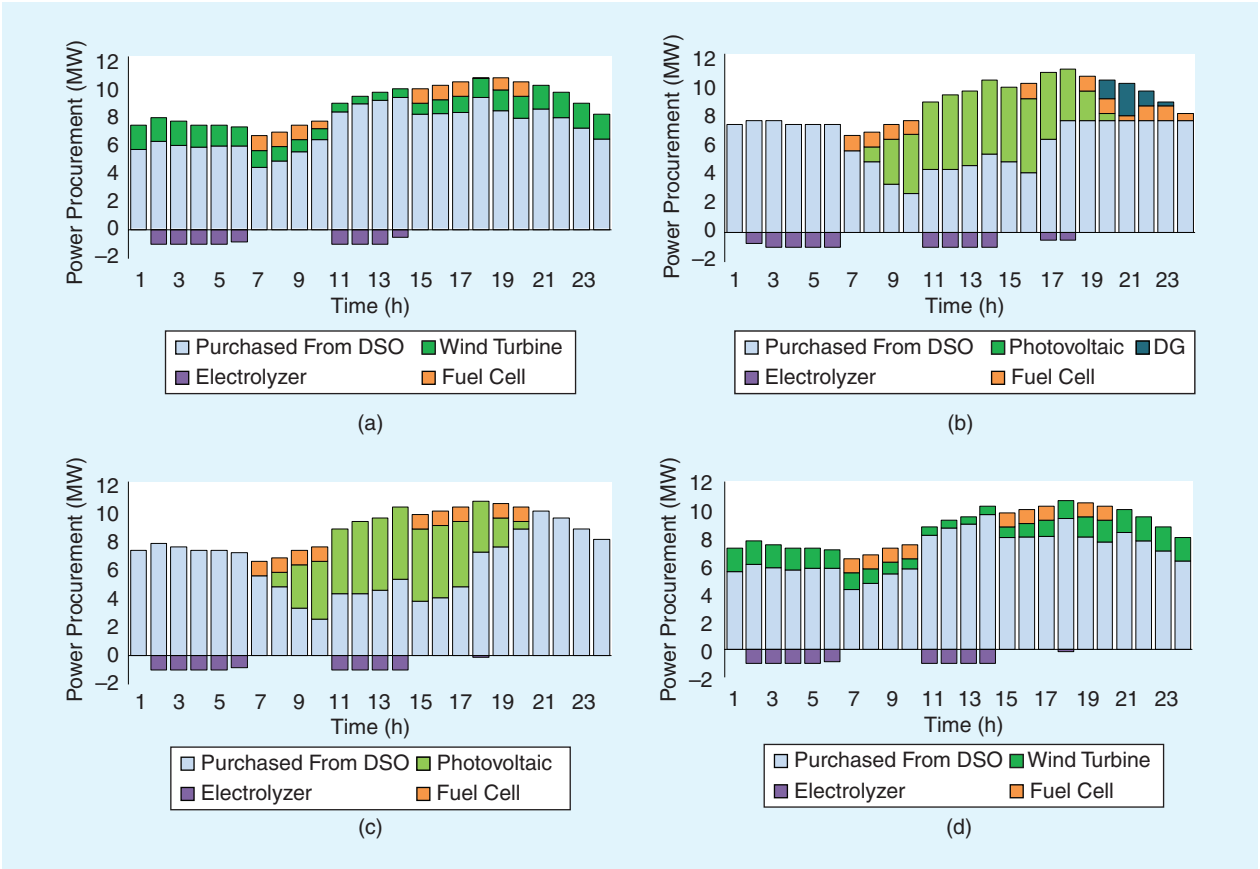

FIGURE 10. Power dispatch in the microgrids. MG: microgrid. (a) MG1, (b) MG2, (c) MG3, and (d) MG4.

the DSO profit, the optimization tried to increase the purchased power from the distribution system. Also, solar photovoltaic generation in MG2 and MG3, and wind generation in MG1 and MG4, are based on the generated and reduced scenarios, respectively. Also, fuel cell power generation, as well as electrolyzers power consumptions, are almost the same in all microgrids as their scheduling is determined by the load patterns, which are similar in all microgrids.

Furthermore, the distributed power generation in MG2 is committed in some high-cost hours while it is not utilized in MG1 as the MGO decides to use the low-price grid power instead of distributed generation's high-cost power. Finally, no loss of load happened in all microgrids because of the high penalty price.

Conclusion

This article proposed a novel bilevel framework in light of the hierarchical nature of decision making and uncertainty to solve the hydrogen-based microgrid operation scheduling problem within the distribution network. The framework was used to model a distribution system in which multiple microgrids exist with uncertainty in the loads, solar, and wind power. Real hourly data of renewable power and load demand were obtained from the CAISO and prepared for scenario reduction. An unsupervised machine learning method was adopted to reduce the initial uncertainty scenarios set to decrease the computational complexity. Based on our research, the following conclusions can be drawn:

- The coordinated model outperformed the centralized model. Moreover, the operation cost of microgrids was almost the same in both models, which verified our model's capabilities.
- The availability of resources determines the price and amount of power between microgrids and distribution systems. The power price of microgrids with adequate power resources is lower than that of microgrids with insufficient resources.
- Hydrogen systems provided an added level of flexibility to the microgrids, which made it possible to manage a surplus of renewable resources.
- The power dispatch in the microgrids was based on the scenarios of uncertain variables and the marginal power price of resources.

All in all, an ISO will be the final user of this study to find the best price and exchange power between two entities. This study provided a comprehensive framework for the DSO and MGOs to cooperate while satisfying their respective objective functions.

Acknowledgment

The work of M.H. Shams and J. Jay Liu was supported by Basic Science Research Program through the National Research Foundation of Korea funded by the Ministry of Science and ICT (2019R1A2C2084709, 2021R1A4A3025742). M.S. Javadi acknowledges FCT for his contract funding provided through 2021.01052.CEECIND. João P.S. Catalão acknowledges support by FEDER funds through COMPETE 2020 and by Portuguese funds through FCT, under POCI-01-0145-FEDER-029803 (02/SAICT/2017). The corresponding authors are J. Jay Liu and João P.S. Catalão.

Author Information

Mohammad H. Shams is with Pukyong National University, Busan 48547 Republic of Korea. ***Mohammad Mansour-Lakouraj*** is with Babol Noshirvani University of Technology, Babol 47148-71167, Iran. ***J. Jay Liu*** (jayliu@pknu.ac.kr) is with Pukyong National University, Busan 48513 Republic of Korea. ***Mohammad S. Javadi*** is with INESC TEC, 4200-465 Porto, Portugal. ***João P.S. Catalão*** (catalao@fe.up.pt) is with the University of Porto and INESC TEC, 4200-465 Porto, Portugal. Javadi is a Senior Member of IEEE. Catalão is a Fellow of IEEE. This article first appeared as "Learning-Based Coordinated Operation of Multiple Microgrids with Hydrogen Systems" (10.1109/SEST50973.2021.9543410) at the 2021 International Conference on Smart Energy Systems and Technologies. This article was reviewed by the IEEE IAS Energy Systems Committee.

References

[1] S. Parhizi, H. Lotfi, A. Khodaei, and S. Bahramirad, "State of the art in research on microgrids: A review," *IEEE Access*, vol. 3, pp. 890–925, Jun. 2015, doi: 10.1109/ACCESS.2015.2443119.

[2] W. Gu et al., "Modeling, planning and optimal energy management of combined cooling, heating and power microgrid: A review," *Int. J. Electr. Power Energy Syst*, vol. 54, pp. 26–37, Jan. 2014, doi: 10.1016/j.ijepes.2013.06.028.

[3] M. Sajawal Akhtar, R. Dickson, H. Niaz, D. W. Hwang, and J. J. Liu, "Comparative sustainability assessment of a hydrogen supply network for hydrogen refueling stations in Korea – A techno-economic and lifecycle assessment perspective," *Green Chem.*, vol. 23, no. 23, pp. 9625–9639, Nov. 2021, doi: 10.1039/D1GC03006J.

[4] M. S. Akhtar, R. Dickson, and J. J. Liu, "Life cycle assessment of inland green hydrogen supply chain networks with current challenges and future prospects," *ACS Sustain. Chem. Eng.*, vol. 9, no. 50, pp. 17,152–17,163, Dec. 2021, doi: 10.1021/ACSSUSCHEMENG.1C06769.

[5] I. Dincer, "Green methods for hydrogen production," *Int. J. Hydrogen Energy*, vol. 37, no. 2, pp. 1954–1971, Jan. 2012, doi: 10.1016/j.ijhydene.2011.03.173.

[6] A. Rabiee, A. Keane, and A. Soroudi, "Green hydrogen: A new flexibility source for security constrained scheduling of power systems with renewable energies," *Int. J. Hydrogen Energy*, vol. 46, no. 37, pp. 19,270–19,284, May 2021, doi: 10.1016/j.ijhydene.2021.03.080.

[7] A. Rabiee, A. Keane, and A. Soroudi, "Technical barriers for harnessing the green hydrogen: A power system perspective," *Renew. Energy*, vol. 163, pp. 1580–1587, Jan. 2021, doi: 10.1016/j.renene.2020.10.051.

[8] B. Frew et al., "The curtailment paradox in the transition to high solar power systems," *Joule*, vol. 5, no. 5, pp. 1143–1167, May 2021, doi: 10.1016/j.joule.2021.03.021.

[9] J. Zheng, A. A. Chien, and S. Suh, "Mitigating curtailment and carbon emissions through load migration between data centers," *Joule*, vol. 4, no. 10, pp. 2208–2222, Oct. 2020, doi: 10.1016/j.joule.2020.08.001.

[10] S. Kharel and B. Shabani, "Hydrogen as a long-term large-scale energy storage solution to support renewables," *Energies*, vol. 11, no. 10, p. 2825, 2018, doi: 10.3390/en11102825.

[11] G. Yang, Y. Jiang, and S. You, "Planning and operation of a hydrogen supply chain network based on the off-grid wind-hydrogen coupling system," *Int. J. Hydrogen Energy*, vol. 45, no. 41, pp. 20,721–20,739, Aug. 2020, doi: 10.1016/j.ijhydene.2020.05.207.

[12] Z. Li and Y. Xu, "Optimal coordinated energy dispatch of a multi-energy microgrid in grid-connected and islanded modes," *Appl. Energy*, vol. 210, pp. 974–986, Jan. 2018, doi: 10.1016/j.apenergy.2017.08.197.

[13] M. H. Shams, M. Shahabi, M. MansourLakouraj, M. Shafie-Khah, and J. P. S. Catalão, "Adjustable robust optimization approach for two-stage operation of energy hub-based microgrids," *Energy*, vol. 222, May 2021, Art. no. 119894, doi: 10.1016/j.energy.2021.119894.

[14] M. H. Shams, M. Shahabi, and M. E. Khodayar, "Risk-averse optimal operation of Multiple-Energy Carrier systems considering network constraints," *Electr. Power Syst. Res.*, vol. 164, pp. 1–10, Nov. 2018, doi: 10.1016/j.epsr.2018.07.022.

[15] M. Yazdani-Damavandi, N. Neyestani, M. Shafie-Khah, J. Contreras, and J. P. S. Catalao, "Strategic behavior of multi-energy players in electricity markets as aggregators of demand side resources using a bi-level approach," *IEEE Trans. Power Syst.*, vol. 33, no. 1, pp. 397–411, Mar. 2017, doi: 10.1109/tpwrs.2017.2688344.

[16] Z. Yi, Y. Xu, J. Zhou, W. Wu, and H. Sun, "Bi-level programming for optimal operation of an active distribution network with multiple virtual power plants," *IEEE Trans. Sustain. Energy*, vol. 11, no. 4, pp. 2855–2869, Oct. 2020, doi: 10.1109/TSTE.2020.2980317.

[17] S. Bahramara, M. Parsa Moghaddam, and M. R. Haghifam, "A bi-level optimization model for operation of distribution networks with microgrids," *Int. J. Electr. Power Energy Syst.*, vol. 82, pp. 169–178, Nov. 2016, doi: 10.1016/j.ijepes.2016.03.015.

[18] G. E. Asimakopoulou, A. L. Dimeas, and N. D. Hatziargyriou, "Leader-follower strategies for energy management of multi-microgrids," *IEEE Trans. Smart Grid*, vol. 4, no. 4, pp. 1909–1916, Dec. 2013, doi: 10.1109/TSG.2013.2256941.

[19] M. Carrión, J. M. Arroyo, and A. J. Conejo, "A bilevel stochastic programming approach for retailer futures market trading," *IEEE Trans. Power Syst*, vol. 24, no. 3, pp. 1446–1456, Aug. 2009, doi: 10.1109/TPWRS.2009.2019777.

[20] Z. Wang, B. Chen, J. Wang, M. M. Begovic, and C. Chen, "Coordinated energy management of networked microgrids in distribution systems," *IEEE Trans. Smart Grid*, vol. 6, no. 1, pp. 45–53, Jan. 2015, doi: 10.1109/TSG.2014.2329846.

[21] H. Golpîra, S. Bahramara, S. A. R. Khan, and Y. Zhang, "Robust bi-level risk-based optimal scheduling of microgrid operation against uncertainty," *RAIRO - Oper. Res.*, vol. 54, no. 4, pp. 993–1012, Jul. 2020, doi: 10.1051/ro/2019046.

[22] M. Mansour-Lakouraj and M. Shahabi, "Comprehensive analysis of risk-based energy management for dependent micro-grid under normal and emergency operations," *Energy*, vol. 171, pp. 928–943, Mar. 2019, doi: 10.1016/j.energy.2019.01.055.

[23] X. Xu, Z. Yan, M. Shahidehpour, Z. Li, M. Yan, and X. Kong, "Data-driven risk-averse two-stage optimal stochastic scheduling of energy and reserve with correlated wind power," *IEEE Trans. Sustain. Energy*, vol. 11, no. 1, pp. 436–447, Jan. 2020, doi: 10.1109/TSTE.2019.2894693.

[24] N. Growe-Kuska, H. Heitsch, and W. Romisch, "Scenario reduction and scenario tree construction for power management problems," in *Proc. IEEE Bologna Power Tech Conf.*, 2003, p. 7, doi: 10.1109/PTC.2003.1304379.

[25] L. Che, X. Zhang, M. Shahidehpour, A. Alabdulwahab, and A. Abusorrah, "Optimal interconnection planning of community microgrids with renewable energy sources," *IEEE Trans. Smart Grid*, vol. 8, no. 3, pp. 1054–1063, May 2017, doi: 10.1109/TSG.2015.2456834.

[26] J. L. Crespo-Vazquez, C. Carrillo, E. Diaz-Dorado, J. A. Martinez-Lorenzo, and M. Noor-E-Alam, "A machine learning based stochastic optimization framework for a wind and storage power plant participating in energy pool market," *Appl. Energy*, vol. 232, pp. 341–357, Dec. 2018, doi: 10.1016/j.apenergy.2018.09.195.

[27] S. Bahramara, P. Sheikhahmadi, A. Mazza, G. Chicco, M. Shafie-Khah, and J. P. S. Catalão, "A risk-based decision framework for the distribution company in mutual interaction with the wholesale day-ahead market and microgrids," *IEEE Trans. Ind. Informat.*, vol. 16, no. 2, pp. 764–778, Feb. 2020, doi: 10.1109/TII.2019.2921790.

[28] M. H. Shams, M. MansourLakouraj, J. J. Liu, M. S. Javadi, and J. P. S. Catalão, "Bi-level two-stage stochastic operation of hydrogen-based microgrids in a distribution system," in *Proc. Int. Conf. Smart Energy Syst. Technol. (SEST)*, 2021, pp. 1–6, doi: 10.1109/SEST50973.2021.9543410.

[29] Z. Deng and Y. Jiang, "Optimal sizing of wind-hydrogen system considering hydrogen demand and trading modes," *Int. J. Hydrogen Energy*, vol. 45, no. 20, pp. 11,527–11,537, Apr. 2020, doi: 10.1016/j.ijhydene.2020.02.089.
[30] F. Khavari, A. Badri, and A. Zangeneh, "Energy management in multi-microgrids via an aggregator to override point of common coupling congestion," *IET Gener. Transmiss. Distrib.*, vol. 13, no. 5, pp. 634–643, 2019, doi: 10.1049/iet-gtd.2018.5922.
[31] "California ISO." Accessed: Nov. 29, 2021. [Online]. Available: https://www.caiso.com/Pages/default.aspx
[32] "SCENRED." GAMS. Accessed: Mar. 30, 2021. [Online]. Available: https://www.gams.com/33/docs/T_SCENRED.html
[33] A. Likas, N. Vlassis, and J. J. Verbeek, "The global k-means clustering algorithm," *Pattern Recognit.*, vol. 36, no. 2, pp. 451–461, Feb. 2003, doi: 10.1016/S0031-3203(02)00060-2.
[34] C. Ruiz, A. J. Conejo, and Y. Smeers, "Equilibria in an oligopolistic electricity pool with stepwise offer curves," *IEEE Trans. Power Syst.*, vol. 27, no. 2, pp. 752–761, May 2012, doi: 10.1109/TPWRS.2011.2170439.
[35] A. V. Fiacco and G. P. McCormick, *Nonlinear Programming: Sequential Unconstrained Minimization Techniques*. Philadelphia, PA, USA: SIAM, 1990.
[36] J. Fortuny-Amat and B. McCarl, "A representation and economic interpretation of a two-level programming problem," *J. Oper. Res. Soc.*, vol. 38, no. 3, pp. 277–286, 1987, doi: 10.1057/jors.1981.156.
[37] "Cutting edge modeling." GAMS. Accessed: Mar. 24, 2021. [Online]. Available: https://www.gams.com/